Journal of Industrial and Engineering Chemistry xxx (xxxx) xxx

Contents lists available at ScienceDirect

Journal of Industrial and Engineering Chemistry

journal homepage: www.elsevier.com/locate/jiec

Interfacial approach to fabricate covalently and noncovalently attached inverse-phosphocholine supported lipid bilayers on TiO_2 and SiO_2 surfaces

Tun Naw Sut [a,b], Sigalit Meker [a], Dong Jun Koo [b], Joshua A. Jackman [b,*], Nam-Joon Cho [a,*]

[a] School of Materials Science and Engineering, Nanyang Technological University, 50 Nanyang Avenue, 639798, Singapore
[b] School of Chemical Engineering and Translational Nanobioscience Research Center, Sungkyunkwan University, Suwon 16419, Republic of Korea

ARTICLE INFO

Article history:
Received 4 May 2023
Revised 6 July 2023
Accepted 24 July 2023
Available online xxxx

Keywords:
Supported lipid bilayer
Inverse-phosphocholine lipid
Solution pH
Ionic strength
Surface functionalization
Quartz crystal microbalance-dissipation

ABSTRACT

Inverse-phosphocholine lipids such as DOCP are intriguing biomolecules for surface functionalization because they can form supported lipid bilayers (SLBs) on titania surfaces but adsorb weakly on silica surfaces. Interestingly, these trends are nearly opposite to those of conventional phosphocholine lipids, motivating deeper investigation of how environmental parameters affect DOCP lipid vesicle adsorption phenomena. Herein, we systematically investigated how solution pH (4, 6, 8, 10) and ionic strength (50, 150, 250 mM NaCl) influence DOCP lipid vesicle adsorption behavior on titania and silica surfaces. On titania, DOCP lipid vesicles either adsorbed and ruptured to form a covalently attached SLB (acidic pH), adsorbed but did not rupture (basic pH with high salt), or did not adsorb (basic pH with low salt). Conversely, on silica, a narrow range of acidic pH, high-salt conditions triggered DOCP lipid vesicle adsorption and rupture to form a noncovalently attached SLB whereas negligible adsorption occurred in other conditions. The corresponding energetics of the vesicle-surface interaction and lipid attachment properties were analyzed and clarify how the interplay of solution pH and ionic strength modulates DOCP lipid vesicle adsorption behavior. Based on these insights, we identified suitable strategies to fabricate covalently and noncovalently stabilized inverse-phosphocholine lipid bilayers on oxide surfaces.

Introduction

Supported lipid bilayers (SLBs) are two-dimensional lipid bilayer interfaces that form on oxide surfaces and are widely used for biomimetic surface functionalization of bulk surfaces and nanoparticles, both in terms of preventing biofouling and improving surface modification possibilities in an orthogonal manner [1–4]. SLB coatings composed of zwitterionic phosphatidylcholine (PC) lipids are the most popular type because they can prevent nonspecific protein adsorption [5] and cell attachment [6]. Typically, the SLB formation process depends on the adsorption and spontaneous rupture of PC lipid vesicles on hydrophilic, silica-based materials like silica and mica [7–9]. The rupture process is principally driven by a sufficiently strong vesicle-substrate interaction that causes deformation of adsorbed vesicles to induce rupture *via* one or more self-assembly pathways [10–12]. However, PC lipid vesicles adsorb but do not rupture on a wide range of metal oxide surfaces, implying that the vesicle-substrate interaction is weaker in those cases [13,14]. One prominent example is titania [15–17], which has broad relevance for medical applications such as implant coatings [18]. To facilitate SLB formation on titania, numerous approaches have been devised to promote vesicle rupture, either through peptide-induced membrane destabilization [19] or by increasing vesicle-substrate interaction strength [20]. The latter approach can be achieved by changing the solution pH [21], adding divalent cations [22], or incorporating charged lipids into the vesicle composition [23–25]. In all these cases, however, the range of suitable lipid compositions is limited and the SLB platforms are weakly attached on account of being stabilized by noncovalent forces alone.

To address these shortcomings, the design of functionalized lipids that enable covalent anchoring of SLBs on titania is an emerging SLB fabrication strategy [26]. Perttu *et al.* reported the synthesis of zwitterionic, inverse-phosphocholine (CP) lipids that – compared to conventional PC lipids – have a reverse charge orientation with the phosphate group pointed outward [27]. This free

* Corresponding authors.
E-mail addresses: jjackman@skku.edu (J.A. Jackman), njcho@ntu.edu.sg (N.-J. Cho).

https://doi.org/10.1016/j.jiec.2023.07.053
1226-086X/

Please cite this article as: T.N. Sut, S. Meker, D.J. Koo et al., Interfacial approach to fabricate covalently and noncovalently attached inverse-phosphocholine supported lipid bilayers on TiO_2 and SiO_2 surfaces, Journal of Industrial and Engineering Chemistry, https://doi.org/10.1016/j.jiec.2023.07.053

phosphate group can covalently attach to various metal oxide nanoparticle surfaces [28,29]. Wang *et al.* first demonstrated the practical utility of coating metal oxide nanoparticles with 2-((2,3-bis(oleoyloxy)propyl)dimethylammonio)ethyl hydrogen phosphate (DOCP) lipids in this class [30]. While DOCP lipids attach to titania surfaces *via* covalent bond formation, these lipids display only weak attachment to silica surfaces [30]. Interestingly, DOCP SLBs can form on a wide range of other types of metal oxide nanoparticles [31] as well as on planar titania surfaces [32–34]. Recent evidence also points to the interplay of covalent and noncovalent forces in dictating the outcome of DOCP lipid vesicle-substrate interactions on titania, *i.e.*, intact vesicle adsorption or SLB formation, while corresponding interactions on silica were generally unfavorable [32].

Motivated by these findings, it is important to determine how environmental factors like solution pH and ionic strength affect DOCP lipid vesicle-substrate interactions and whether modulating such factors might overcome apparent surface specificities and enable DOCP SLB formation on silica surfaces as well. Indeed, in addition to serving as durable coatings for biosensing and medical implant applications [33], CP lipid-based coatings are receiving industrial attention as biocompatible drug delivery vehicles and coatings amenable to surface modification [35–38] and click chemistry *in vivo* [39], as well as surface coatings for organic and inorganic theragnostic and imaging probes [31,40]. As silica is an important material for biomedical applications, demonstrating the feasibility to fabricate CP-based SLBs on silica surfaces would establish an important proof-of-principle while further laying the groundwork to expand the usage of DOCP lipid bilayer coatings in different application settings.

The aim of the present study was to systematically investigate how solution pH and ionic strength influence DOCP lipid vesicle adsorption onto titania and silica surfaces. Quartz crystal microbalance-dissipation (QCM-D) measurements were conducted to measure vesicle adsorption kinetics and to characterize the mass and viscoelastic properties of DOCP lipid assemblies. The QCM-D experiments were complemented by analytical modeling based on extended-DLVO (E-DLVO) theory to further analyze the contribution of noncovalent lipid-substrate interactions in mediating the initial adsorption step. This interfacial science approach led us to identify suitable conditions to form covalently and noncovalently attached DOCP SLBs on titania and silica surfaces, respectively, and we also discuss the corresponding role of noncovalent interactions in driving spontaneous vesicle rupture along with different lipid attachment mechanisms.

Materials and methods

Sample preparation

2-((2,3-bis(oleoyloxy)propyl)dimethylammonio)ethyl hydrogen phosphate (DOCP) and 1,2-dioleoyl-*sn*-glycero-3-phosphocholine (DOPC) lipid stocks in chloroform were obtained from Avanti Polar Lipids, Inc. (Alabaster, AL) and stored at −20 °C. DOCP and DOPC lipid vesicles were prepared by the extrusion method [41]. Briefly, a dried lipid film of specified composition was prepared and then hydrated in an aqueous buffer (10 mM Tris, pH 7.5 with specified NaCl concentration) to a 5 mg/mL lipid concentration, followed by vortexing for 3 min. Vesicles were then extruded with a Mini-Extruder (Avanti Polar Lipids) through a polycarbonate membrane with 50 nm-diameter pores. Before experiment, the stock vesicles were diluted to 0.1 mg/mL lipid concentration in the appropriate buffer solution. All buffer solutions were prepared with 10 mM Tris using Milli-Q-treated water (>18 MΩ·cm) (Millipore, Billerica, MA) and had 50, 150, or 250 mM NaCl salt concentrations as specified. Solution pH adjustment was done by adding NaOH or HCl as applicable and verified by potentiometric pH measurement (Lab 845, SI Analytics, Washington, DC) during preparation and again immediately before experiment.

Vesicle characterization

The size distribution of DOCP lipid vesicles was measured by the dynamic light scattering (DLS) technique using a 90Plus particle size analyzer (Brookhaven Instruments Corporation, Holtsville, NY), as previously described [42], and the intensity-weighted size distributions are reported. To assess vesicle stability, vesicle size was measured as a function of incubation time and t = 0 min indicates the time when the vesicles were diluted initially in applicable cases. The zeta potential values of DOCP lipid vesicles were also measured in different buffer solutions by using an ELSZ-2000 instrument (Otsuka Electronics Co., Ltd, Osaka, Japan). Each measurement set included 2 readout cycles with 10 accumulated readings per cycle at a sampling rate of 400 μs/reading. For experiments, the vesicle samples were diluted to 0.1 mg/mL lipid concentration in the appropriate buffer solution.

Quartz crystal microbalance-dissipation (QCM-D)

QCM-D measurements were performed with a Q-Sense E4 instrument (Biolin Scientific AB, Gothenburg, Sweden) to monitor vesicle adsorption kinetics onto titania and silica surfaces, as previously described [32]. Sputter-coated, 5 MHz crystals with 50-nm-thick silica or titania layers (QSX no. 303 and 310, Biolin Scientific AB) were used for all measurements. It has been previously reported that the silica coating is amorphous while the titania coating is mainly in the anatase phase [43]. Atomic force microscopy (AFM) experiments have shown that the root-mean-square roughness of both sensor surfaces is ∼0.5 nm (see Refs. [15,44]). Before experiment, the surfaces were rinsed with water and ethanol, dried with nitrogen gas, and treated with oxygen plasma by using an Expanded Plasma Cleaner (PDC-002, Harrick Plasma, Ithaca, NY). Liquid samples were injected into the measurement chambers at a 50 μL/min rate by a peristaltic pump (Reglo Digital, Ismatec, Glattbrugg, Switzerland). The temperature in the measurement chambers was maintained at 25 °C throughout the experiments. The temporal changes in QCM-D resonance frequency (Δf) and energy dissipation (ΔD) signal were tracked at odd overtones and the normalized data at the 5th overtone are presented. In applicable cases where SLB formation occurred, the adlayer thickness was further estimated by applying the Sauerbrey equation [7] and taking into account the DOCP lipid molecular weight (772 Da) along with estimated headgroup area (0.68 nm^2) and length (1.85 nm) [45].

Results and discussion

Vesicle adsorption kinetics

The surface-sensitive QCM-D technique was selected for tracking lipid vesicle adsorption onto the different oxide surfaces because it is label-free, has sufficiently fast time resolution, and is highly sensitive to the amount and structural configuration of adsorbed lipid molecules and hydrodynamically coupled solvent molecules [46]. This sensitivity is particularly noteworthy when compared to other options such as the refractometric-based surface plasmon resonance (SPR) and localized surface plasmon resonance (LSPR) techniques that are sensitive to the mass of adsorbed lipid molecules only and do not detect hydrodynamically coupled solvent [47]. In past works, the QCM-D technique has demon-

strated versatility to detect different pathways of lipid vesicle adsorption onto surfaces, such as one- and two-step SLB formation, irreversible and reversible intact vesicle adsorption, and negligible adsorption [12,48].

To monitor DOCP lipid vesicle adsorption in different pH and ionic strength conditions, QCM-D experiments were performed on titania- and silica-coated sensor surfaces, and changes in resonance frequency (Δf) and energy dissipation (ΔD) signals due to vesicle adsorption processes were temporally tracked [49]. Δf is related to the acoustic mass of adsorbed lipids while ΔD is sensitive to the adsorbate's viscoelastic properties [50]. Operationally, a baseline signal was first established in aqueous buffer solution for 5 min before adding 0.1 mg/mL, ~70-nm diameter DOCP lipid vesicles in equivalent buffer solution. After the adsorption behavior stabilized, a buffer washing step (without vesicles) was performed. The final Δf and ΔD shifts after buffer washing are reported below.

In general, complete SLB formation was determined by Δf and ΔD shift values in the range of −25 Hz and $< 1 \times 10^{-6}$, respectively, relative to the buffer baseline values [50]. These values correspond to a complete, rigid (non-viscoelastic) SLB coating, which makes it possible to extract the areal mass density according to the Sauerbrey model (~440 ng/cm^2) and agrees well with theoretical estimates of a lipid bilayer packing with ~ 100% surface coverage that take into account lipid headgroup area and molecular weight, as previously discussed [7]. One-step SLB formation kinetics further indicate particularly strong vesicle-surface interactions where individual vesicles can rupture upon adsorption, whereas two-step SLB formation kinetics indicate that vesicle rupture only commenced after a critical surface coverage of adsorbed vesicles was reached and that a combination of vesicle-surface and vesicle-vesicle interactions was needed to trigger rupture [13]. Both one-step and two-step formation kinetics lead to SLBs of equivalent quality; the main difference lies in the vesicle-surface interaction strength needed to trigger vesicle rupture. On the other hand, intact vesicle adsorption was determined by Δf and ΔD shift values in excess of −60 Hz and $> 3 \times 10^{-6}$, respectively, relative to the buffer baseline values. The high energy dissipation in this case corresponds to a viscoelastic adlayer, which is characteristic of intact vesicle adlayers with coupled solvent inside the vesicle interiors and in between the vesicles [51]. Also, the vesicle adsorption kinetics showed monotonic behavior. In addition, negligible vesicle adsorption was determined by Δf and ΔD shift values of less than −2 Hz and $\sim 0.5 \times 10^{-6}$, respectively, relative to the buffer baseline values.

Before the QCM-D experiments, we also characterized the size and charge properties of the extruded DOCP lipid vesicles in bulk solution. Dynamic light scattering (DLS) measurements indicated that the vesicles had ~ 70-nm diameter and zeta potential measurements confirmed the expected negative charge, the magnitude of which varied depending on the test condition. The corresponding values were around −22 to −44 mV, −27 to −43 mV, −28 to −46 mV, and −42 to −58 mV at pH 4, 6, 8, and 10, respectively as the ionic strength increased from 50 to 250 mM NaCl (**Fig. S1**). The specific charge of the titania and silica surfaces also depended on the solution pH as discussed below.

pH 4

We first investigated DOCP lipid vesicle adsorption onto titania surfaces in pH 4 conditions. At 50 mM NaCl, one-step adsorption kinetics were observed (Fig. 1**A**). The final Δf and ΔD shifts were consistently around −23.2 ± 2.3 Hz and 0.3 ± 0.4 × 10^{-6}, respectively, and indicate successful SLB formation (~4.0 nm thickness) [50]. The one-step kinetics support that individual vesicles rupture spontaneously upon adsorption. This observation fits with the net-positive charge of titania surfaces below its isoelectric point [52,53] and is also consistent with past reports of strong DOCP lipid binding to titania nanoparticles in this pH regime [30].

Interestingly, at 150 mM NaCl, two different adsorption profiles were observed variably (Fig. 1**B**). In one case, the measurement responses pointed to SLB formation with one-step adsorption kinetics, as demonstrated by final Δf and ΔD shifts around −26.0 ± 1.7 Hz and 0.2 ± 0.3 × 10^{-6}, respectively, corresponding to ~4.5 nm thickness (Fig. 1**B**, solid line). In the other case, the adsorption kinetics showed more complex behavior, indicating greater lipid adsorption with final Δf and ΔD shifts around −54.1 ± 5.4 Hz and 8.0 ± 1.8 × 10^{-6}, respectively (Fig. 1**B**, dashed line). Both kinetic profiles were repeatedly observed, and this variable interaction behavior was attributed to aggregation of solution-phase vesicles, as indicated by DLS experiments (**Fig. S2** and **Supplementary Discussion**). Since hydronium ions can form strong, long-lived hydrogen bonds with multiple phosphate groups [54] and hence act like a bridging ligand, it is plausible that the unique molecular features of the DOCP lipid headgroup (*i.e.*, phosphate group pointed outwards from the vesicle surface) contribute to hydronium ion-induced vesicle aggregation. Notably, the extent of vesicle aggregation occurs in an ionic strength-dependent manner, whereby a higher bulk NaCl salt concentration translates into more sodium ions competitively binding in a monovalent manner to the phosphate groups [55] of the DOCP lipid vesicle surface and hence less vesicle aggregation occurs. In addition to the aforementioned cases, at 250 mM NaCl, one-step adsorption kinetics were consistently observed and final Δf and ΔD shifts of −26.2 ± 0.9 H z and 0.2 × 10^{-6}, respectively, indicate SLB formation (~4.6 nm thickness) (Fig. 1**C**). Altogether, the results support that SLB formation occurs on titania at pH 4 largely independently of ionic strength, and it is preferable to use relatively low (50 mM NaCl) or high (250 mM NaCl) salt concentrations for reproducibility.

Conversely, on silica, we observed that DOCP lipid vesicle adsorption was negligible at 50 mM NaCl, with final Δf and ΔD shifts of −1.8 ± 0.6 Hz and 0.6 ± 0.5 × 10^{-6}, respectively (Fig. 1**D**). Since silica has an isoelectric point around pH 2 (ref. [56]), it has a negative surface charge at pH 4, which contributes to electrostatic repulsion with negatively charged DOCP lipid vesicles. With increasing salt concentration, greater charge-shielding can occur and vesicle adsorption was observed at 150 mM NaCl (Fig. 1**E**). As with the titania case, multiple adsorption profiles were observed at this ionic strength condition due to vesicle instability, including two-step vesicle adsorption and spontaneous rupture. In that case, the final Δf and ΔD shifts were −28.0 ± 0.0 Hz and 0.4 ± 0.0 × 10^{-6}, respectively, which are generally consistent with SLB formation (~4.9 nm thickness) (Fig. 1**E**, solid line) [50,57]. In the other two cases, intact vesicle adsorption or incomplete rupture of adsorbed vesicles occurred, and the typical ranges of Δf and ΔD shifts in those cases were around −85.2 ± 14.9 Hz and 20.3 ± 4.4 × 10^{-6}, respectively (Fig. 1**E**, dashed and dotted lines).

At 250 mM NaCl, SLB formation was observed consistently with two-step adsorption kinetics yielding final Δf and ΔD shifts of −25. 0 ± 0.1 Hz and 0.1 ± 0.1 × 10^{-6}, respectively (Fig. 1**F**). These values are within the optimal range for fabricated SLBs [50], likely due to more favorable vesicle-substrate interactions in this condition that facilitate efficient vesicle rupture. As such, the results show that it is possible to form DOCP SLBs on silica under acidic conditions and the efficiency of vesicle adsorption and spontaneous rupture, and consequently SLB formation, improves at higher ionic strengths due to more favorable vesicle-substrate interactions.

pH 6

At pH 6, SLB formation with one-step adsorption kinetics occurred on titania in all tested ionic strength conditions (Fig. 2-**A-C**). At 50 mM NaCl, the final Δf and ΔD shifts were about −23. 9 ± 1.4 Hz and 0.1 ± 0.1 × 10^{-6}, respectively, corresponding

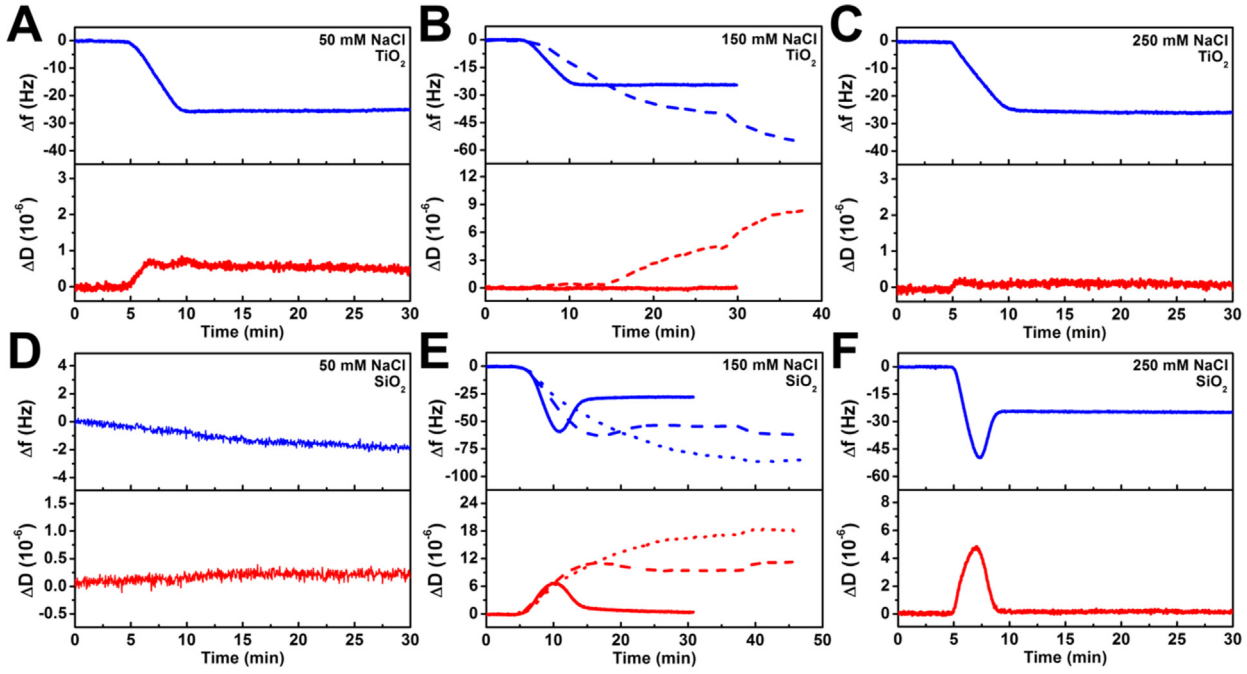

Fig. 1. QCM-D tracking of DOCP lipid vesicle adsorption at pH 4. Frequency, Δf, (blue line) and energy dissipation, ΔD, (red line) shifts were monitored as a function of time in the presence of the following NaCl salt concentrations: **(A)** 50 mM NaCl, **(B)** 150 mM NaCl, and **(C)** 250 mM NaCl on titania, and **(D)** 50 mM NaCl, **(E)** 150 mM NaCl, and **(F)** 250 mM NaCl on silica. Vesicles were added starting at t = 5 min and the baseline values were recorded in equivalent buffer solution without vesicles. The last 10-min duration of the presented time scale in each graph corresponds to a buffer washing step. For panels B and E (150 mM NaCl case), multiple adsorption profiles were observed and each one is plotted with a different line style (solid, dashed, dotted).

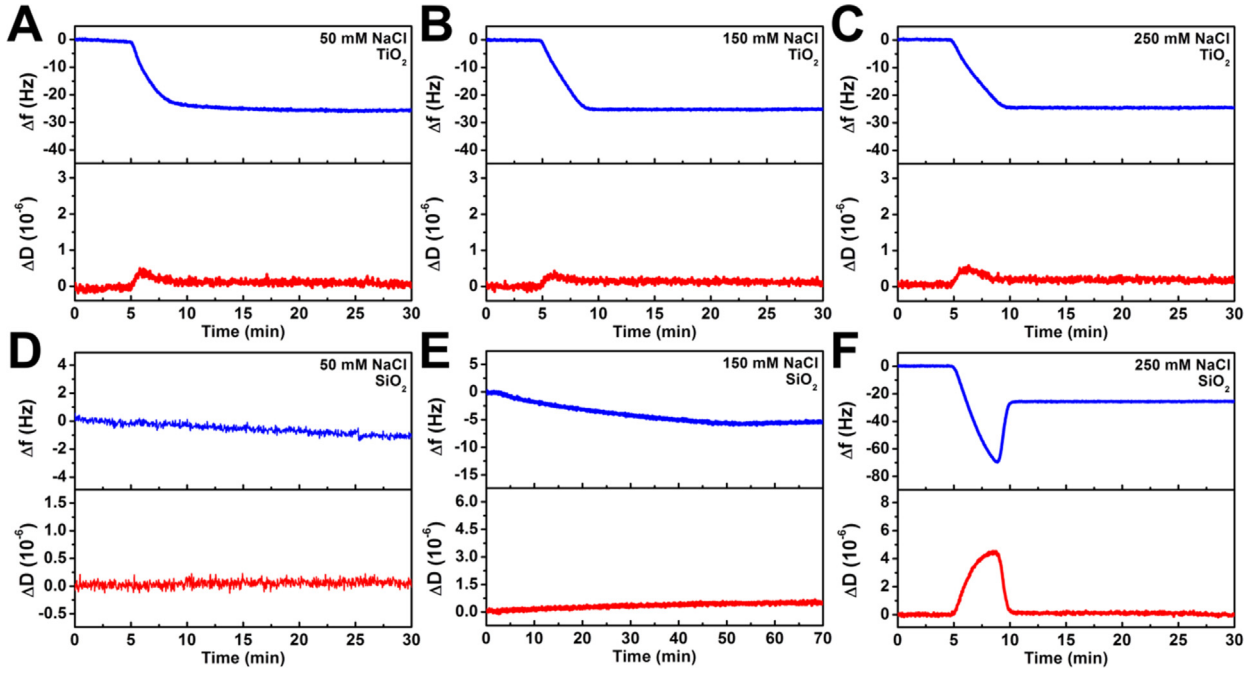

Fig. 2. QCM-D monitoring of DOCP lipid vesicle adsorption at pH 6. The panels are depicted as in Fig. 1.

to ~4.2 nm SLB thickness. Similar values were obtained at higher ionic strengths as well. The final Δf and ΔD shifts were −25.4 ± 0.2 Hz and 0.1 ± 0.1 × 10^{-6}, respectively, at 150 mM NaCl, corresponding to ~4.4 nm SLB thickness, and −25.6 ± 0.8 Hz and 0.2 ± 0.1 × 10^{-6}, respectively, at 250 mM NaCl, corresponding to ~4.4 nm SLB thickness. The results indicate that vesicle-substrate interactions at pH 6 are sufficiently strong to promote DOCP lipid vesicle rupture on titania and this pH condition is highly efficient for fabricating DOCP SLBs. This observation is also consistent with the near-neutral charge of the titania surface since pH 6 is around its isoelectric point [52,53].

On the other hand, at 50 mM NaCl, there was negligible DOCP lipid vesicle adsorption onto silica surfaces with final Δf and ΔD shifts of −0.9 ± 0.2 Hz and 0.1 ± 0.1 × 10^{-6}, respectively (Fig. 2**D**).

At 150 mM NaCl, there was moderate, though still low, adsorption with final Δf and ΔD shifts of −8.6 ± 2.4 Hz and 0.7 ± 0.4 × 10^{-6}, respectively (Fig. 2**E**). Interestingly, at 250 mM NaCl, there was vesicle adsorption and spontaneous rupture after reaching a critical surface coverage of adsorbed vesicles (Fig. 2**F**). The final Δf and ΔD shifts were −25.2 ± 0.5 Hz and 0.1 ± 0.2 × 10^{-6}, respectively, which indicate successful SLB formation (∼4.4 nm thickness). Altogether, the results show that DOCP lipid vesicle adsorption onto silica at pH 6 is strongly dependent on the ionic strength condition, and SLB formation is possible only at high ionic strength conditions (*e.g.*, 250 mM NaCl). Considering the wide spectrum of interaction types observed on silica at pH 6 (no adsorption, weak vesicle adsorption, SLB formation), the data support that charge-shielding plays an important role in modulating the vesicle-substrate interaction strength and corresponding self-assembly behavior of DOCP lipid assemblies on silica.

pH 8

On titania, we discovered that DOCP lipid vesicle adsorption at pH 8 is particularly sensitive to the ionic strength condition, which likely relates to a greater negative charge of the titania surface and corresponding charge-shielding effects. At 50 mM NaCl, there was no vesicle adsorption on titania, as indicated by Δf and ΔD shifts of −0.2 ± 0.2 Hz and 0.0 × 10^{-6}, respectively (Fig. 3**A**). On the other hand, at 150 mM NaCl, DOCP lipid vesicle adsorption and spontaneous rupture occurred after reaching a critical coverage, and SLB formation occurred with final Δf and ΔD shifts of −26.9 ± 1.6 Hz and 0.2 ± 0.1 × 10^{-6}, respectively, corresponding to ∼4.7 nm thickness (Fig. 3**B**). Likewise, at 250 mM NaCl, SLB formation also occurred with final Δf and ΔD shifts of −27.0 ± 0.7 Hz and 0.2 ± 0.3 × 10^{-6}, respectively, corresponding to ∼4.7 nm thickness (Fig. 3**C**). Of note, the SLB formation kinetics were more complex in the latter case and exhibited a broader Δf and a multi-step ΔD response. Hence, DOCP SLBs can be formed on titania at pH 8 in relatively high ionic strength concentrations, whereas essentially no adsorption occurs at lower ionic strength conditions. These findings expand on past titania nanoparticle experiments that noted weak DOCP lipid attachment in the pH ≥ 7 regime [30] and reinforce the importance of modulating the electrostatic force magnitude.

By contrast, on silica, DOCP lipid vesicle adsorption at pH 8 was negligible across all tested ionic strength conditions (Fig. 3**D-F**). The corresponding Δf and ΔD shifts were around −0.1 to −0.3 ± 0.5 Hz and 0.0 × 10^{-6}, respectively. This finding is consistent with past silica nanoparticle studies conducted at pH 7.5 (ref. [30]) and likely relates to strong electrostatic repulsion between the negatively charged DOCP lipid vesicles and silica surface.

pH 10

At pH 10, there was negligible DOCP lipid vesicle adsorption on titania in 50 mM NaCl, as indicated by final Δf and ΔD shifts of −1.0 ± 1.2 Hz and 0.2 ± 0.2 × 10^{-6}, respectively (Fig. 4**A**). With increasing ionic strength, there was greater vesicle adsorption but still no rupture. At 150 mM NaCl, vesicle adsorption occurred and the final Δf and ΔD shifts were −61.3 ± 3.6 Hz and 3.6 ± 0.4 × 10^{-6}, respectively (Fig. 4**B**). At 250 mM NaCl, even greater vesicle adsorption occurred, as indicated by higher Δf and ΔD shifts of −113.4 ± 1.8 Hz and 7.5 ± 0.3 × 10^{-6}, respectively (Fig. 4**C**). Time-independent plots of the Δf and ΔD shifts indicated that deformation of adsorbed vesicles is greater in the pH 10, 150 mM NaCl condition than in the pH 10, 250 mM NaCl condition, which is consistent with less vesicle adsorption (due to more spreading per vesicle) and fits with the overall trend in pH- and ionic strength-dependent effects (**Fig. S3**). Taken together, the results demonstrate that pH 10 is not suitable for forming DOCP SLBs on titania although it is possible to form intact vesicle adlayers in this regime at higher ionic strength conditions. These findings also support that the titania surface has a high negative charge at pH 10 and hence charge-shielding helps to attenuate the degree of electrostatic repulsion but SLB formation is still impeded. Of note, vesicle adsorption occurred until reaching saturation so the surface coverage is likely at most in the range of ∼54%, which is around the jamming limit [58], but such coatings are not useful for surface functionalization on account of low stability (weak vesicle-surface interaction) and inferior coverage (in contrast to the fabricated SLBs, which have ∼100% surface coverage based on the Sauerbrey modeling analysis).

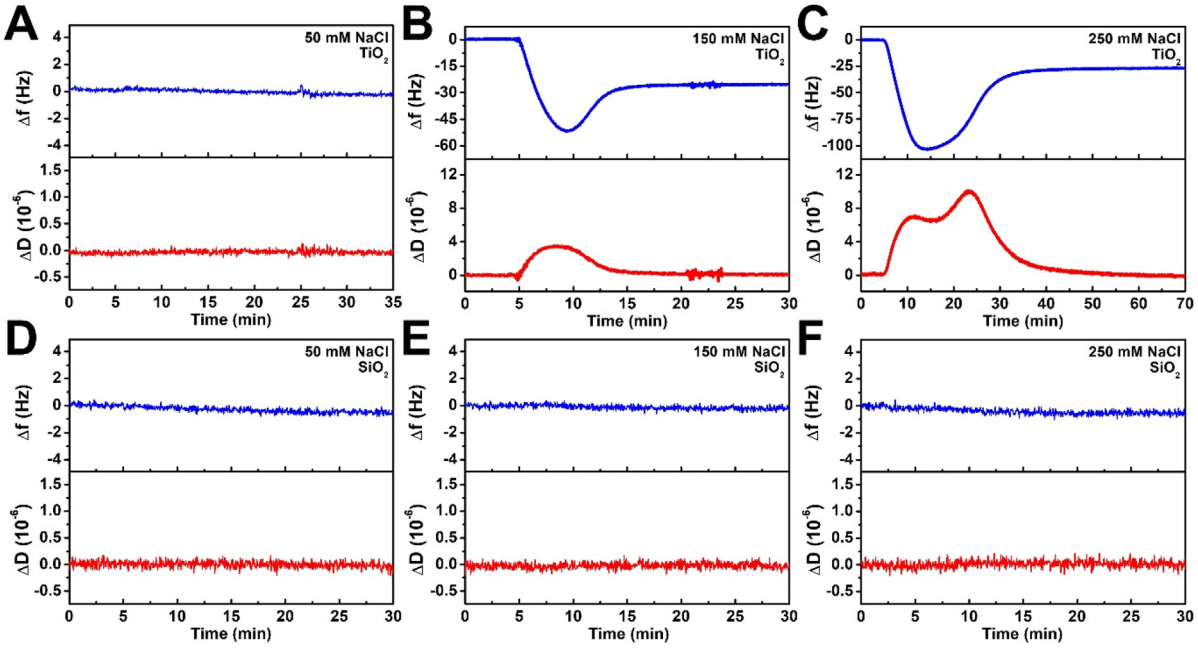

Fig. 3. QCM-D monitoring of DOCP lipid vesicle adsorption at pH 8. The panels are depicted as in Fig. 1.

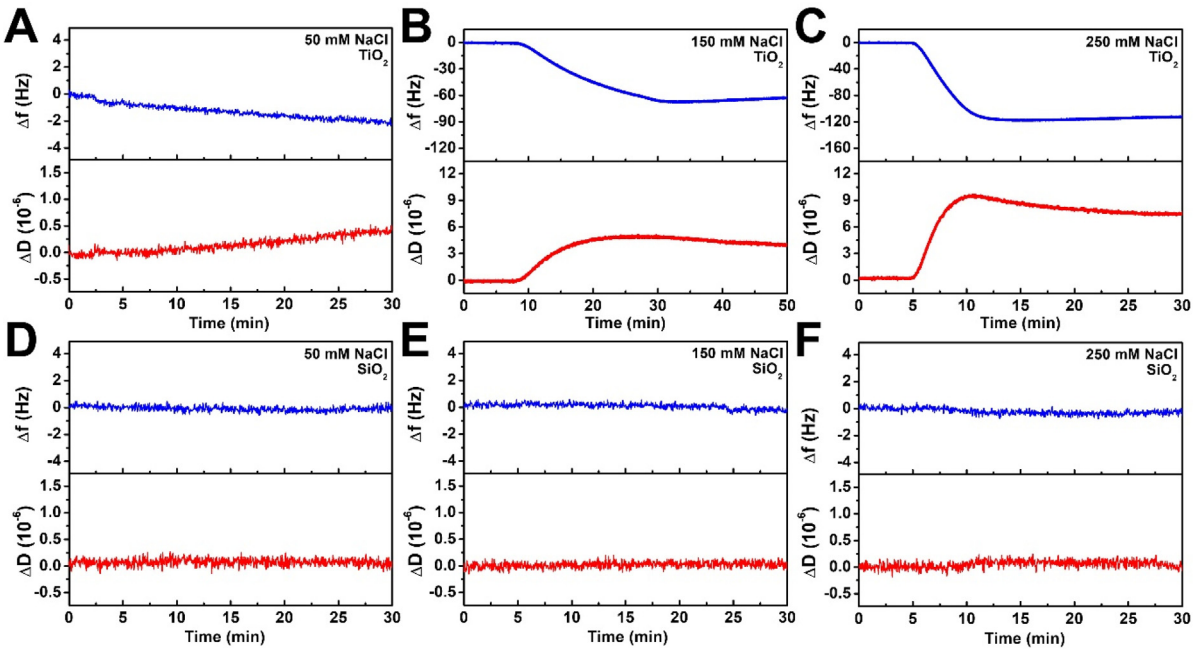

Fig. 4. QCM-D monitoring of DOCP lipid vesicle adsorption at pH 10. The panels are depicted as in Fig. 1.

On the other hand, at pH 10, DOCP lipid vesicle adsorption onto silica was negligible across all tested ionic strength conditions and consistent with the data obtained at pH 8 (Fig. 4**D-F**). The final Δf and ΔD shifts were around −0.1 to −0.8 ± 0.7 Hz and 0.0 to 0.1 ± 0.1 × 10^{-6}, respectively. Hence, DOCP lipid adsorption does not occur onto silica at pH 10 under the tested ionic strength conditions.

Taken together, these findings support that SLB formation can generally occur on titania at pH 4 and 6 and only in higher ionic strength conditions at pH 8, whereas there is only intact vesicle adsorption in high ionic strength conditions at pH 10 (see also **Table S1**). Conversely, SLB formation on silica can also occur in high strength conditions at pH 4 and 6, but no adsorption occurs at pH 8 or 10. These results indicate that DOCP SLB formation is possible on titania and silica surfaces under specific conditions, which led us to investigate the energetic basis for the initial vesicle-surface interaction and post-fabrication stability of attached DOCP lipid molecules.

Vesicle-surface interaction energy analysis

The interaction of negatively charged DOCP lipid vesicles with titania and silica surfaces was further analyzed by considering the interplay of different noncovalent forces that mediate the initial adsorption step, namely the van der Waals, double-layer electrostatic, and steric-hydration forces according to extended-DLVO (E-DLVO) theory [15,57,59,60]. Specifically, the vesicle-substrate contact region was modeled as two planar sheets and the total vesicle-surface interaction energy was calculated as a function of the separation distance between the bilayer and oxide surface in different pH and ionic strength conditions, as previously described [32] (Fig. 5**A**). Across this pH range, the titania surface tended to shift from positive to negative surface charge while silica was always negative [15,59] and the magnitude of the surface potential also varied according to the ionic strength due to charge shielding (**Table S2**). Following this approach, we plotted the total interaction energy as a function of separation distance in order to identify the minimum interaction energy, *i.e.*, the most stable configuration, corresponding to the equilibrium separation distance in each case.

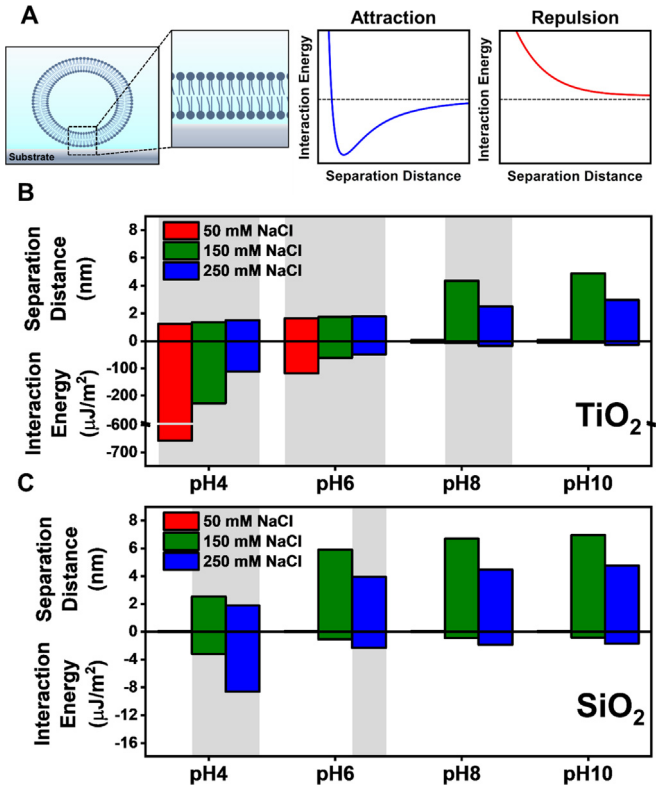

Fig. 5. Interfacial force modeling of DOCP lipid vesicle-surface interaction energy. (A) Schematic illustration of vesicle-surface contact region and representative plots of vesicle-surface interaction energy as a function of separation distance based on E-DLVO theory. Attractive lipid interactions relate to an energy minimum that corresponds to an equilibrium separation distance, whereas there is no energy minimum in cases of repulsive lipid interactions. Calculated values of the equilibrium separation distance and interaction energy in all tested pH and ionic strength conditions for contacting DOCP lipid vesicles on **(B)** titania and **(C)** silica surfaces. The shaded regions correspond to the conditions in which SLBs form based on the QCM-D data.

On titania, the minimum interaction energy for contacting DOCP lipid vesicles at pH 4 was around −657, −228, and −112 μJ/m^2 in 50, 150, and 250 mM NaCl conditions, respectively (Fig. 5**B**). The corresponding equilibrium separation distances were around 1.3–1.5 nm. The smaller interaction energy at higher ionic strength relates to the positive charge of titania, whereby charge shielding decreases electrostatic attraction. Likewise, the minimum interaction energy at pH 6 was around −117, −61, and −49 μJ/m^2 in 50, 150, and 250 mM NaCl conditions, respectively, and the corresponding equilibrium separation distances were around 1.6–1.8 nm. According to the QCM-D data, vesicle rupture with one-step occurred in all of these cases, which supports that the vesicle-surface interactions are sufficiently strong to facilitate vesicle rupture.

On the other hand, at pH 8, unstable interactions were predicted for the 50 mM NaCl condition, which agreed with negligible vesicle adsorption detected in the QCM-D measurements, while the minimum interaction energy was around −7 and −17 μJ/m^2 in 150 and 250 mM NaCl conditions, respectively. In the latter two conditions indicating modestly favorable interactions, the QCM-D experimental results were in good agreement and vesicle rupture with two-step kinetics was observed. In addition, the predicted equilibrium separation distances were around 4.4 and 2.5 nm in 150 and 250 mM NaCl, respectively, indicating that this range of conditions was around a transition point whereby lipid-substrate interactions became more favorable at higher ionic strength. A similar trend occurred at pH 10, in which case unstable interactions were predicted for the 50 mM NaCl condition and no adsorption was observed experimentally as well. In this case, the minimum interaction energy was around −6 and −13 μJ/m^2 in 150 and 250 mM NaCl conditions, respectively, with corresponding equilibrium separation distances around 4.9 and 3.0 nm, and intact vesicle adsorption without rupture occurred in the QCM-D experiments. Together, these data support that one-step vesicle rupture occurred when the minimum interaction energy was around at least −50 μJ/m^2, indicating that sufficiently strong vesicle-substrate interactions in this range can promote spontaneous vesicle rupture. On the other hand, when vesicle-substrate interactions were still favorable but to a lesser extent, two-step vesicle rupture or intact vesicle adsorption without rupture occurred in a pH-dependent manner.

Conversely, on silica, vesicle rupture occurred in only a narrow range of pH and ionic strength conditions (Fig. 5**C**). At pH 4, unstable interactions were predicted for 50 mM NaCl, in which case no adsorption occurred experimentally. By contrast, the minimum interaction energy was around −3 and −9 μJ/m^2 in 150 and 250 mM NaCl conditions, respectively, and the corresponding equilibrium distances were around 2.5 and 2 nm. These values suggest favorable interactions that are consistent with two-step vesicle rupture observed in the QCM-D experiments. At pH 6, an unstable interaction was predicted in 50 mM NaCl, which corresponded to the experimentally observed lack of vesicle adsorption. On the other hand, slightly favorable interactions were predicted in 150 and 250 mM NaCl conditions with corresponding minimum interaction energy values around −1 and −2 μJ/m^2, and the equilibrium separation distances were around 5.9 and 4 nm, respectively. Experimentally, moderate vesicle adsorption and two-step vesicle rupture occurred in 150 and 250 mM NaCl conditions, respectively, which fit the predicted trend in vesicle-surface interaction energy.

Meanwhile, at pH 8, unstable interactions were predicted in 50 mM NaCl, which agrees well with the observation of no vesicle adsorption in the QCM-D experiments, whereas slightly more favorable, but still very weak, interactions were predicted with minimum interaction energy values of around −1 and −2 μJ/m^2 in 150 and 250 mM NaCl conditions, respectively. However, the corresponding separation distances in those cases were around 6.7 and 4.5 nm, which are larger than those at pH 4 and pH 6, and indicative of greater electrostatic repulsion and match trendwise with the experimentally observed lack of vesicle adsorption in both conditions. A similar trend was expected for pH 10 since the calculated values of minimum interaction energy and equilibrium separation distance in all NaCl conditions were almost the same with those at pH 8, which agrees with the lack of adsorption observed in the corresponding QCM-D experiments as well. Altogether, these data show that a minimum interaction energy around −2 to −3 μJ/m^2 is required for two-step vesicle rupture on silica surfaces.

Due to distinct surface hydration properties of the two oxide surfaces as discussed below, it is preferable to analyze the quantitative estimates captured in the interfacial force modeling calculations for each oxide surface independently. In terms of qualitative trends that can be generalized across the two surfaces, the calculation results support that an attractive vesicle-surface interaction energy is needed for DOCP lipid vesicle adsorption and/or rupture to form an SLB while negligible adsorption will occur otherwise. While DOCP SLB formation on titania surfaces is understood to involve covalent bond formation, these findings support that non-covalent interfacial forces are still critical determinants of the initial vesicle-surface interaction on titania and silica surfaces.

Evaluation of lipid anchoring

We also investigated the physical stability of DOCP lipid assemblies by performing an ethanol rinse after vesicle adsorption (except in cases where vesicle adsorption did not occur) was completed to remove noncovalently attached lipid molecules. If a covalently attached monolayer remains, then the final Δf shift is expected to be around −10 to −15 Hz (an ideal monolayer for octadecylmercaptan on gold is approximately −13 Hz) and the ΔD shift should be less than ∼1 × 10^{-6} due to the adsorbate's non-viscoelastic, rigid character [7]. As shown in Fig. 6**A**, the final Δf shifts for DOCP lipid assemblies on titania were almost always within this range, indicating strong lipid-surface attachment. Interestingly, even when DOCP lipid vesicles adsorbed but did not rupture at pH 10, the final Δf shifts were similar to the SLB cases, suggesting that there was still strong attachment but the vesicle-surface interaction strength was insufficient to promote vesicle rupture.

On the other hand, there was no monolayer formation on silica and the final Δf shifts after ethanol washing were appreciably smaller in most cases (Fig. 6**B**). In cases where DOCP lipid adsorption occurred, the final Δf shifts were −8 Hz or smaller except for the anomalous case at pH 4, 150 mM NaCl as described above. Taken together, the experimental data support that the mode of DOCP lipid anchoring and hence SLB stabilization varies on titania *versus* silica surfaces.

While the protein- and cell-related antifouling properties of DOCP-anchored lipid bilayer coatings have been previously discussed in the context of titania surfaces [32,34], we further investigated whether the fabricated DOCP SLBs on titania and silica surfaces could also inhibit biological nanoparticle-related fouling in the present context (**Fig. S4**). Accordingly, DOCP SLBs were fabricated on titania and silica surfaces under suitable fabrication conditions (pH 4, 250 mM NaCl for both cases), followed by solvent-exchange to pH 7.5, 150 mM NaCl. Zwitterionic, ∼70-nm DOPC lipid vesicles generally representative of the size of membrane-enveloped biological nanoparticles like viruses and exosomes were then added to the DOCP SLB-coated surfaces, along with bare surfaces as controls. It was determined that the DOCP SLB coatings fully prevented nonspecific DOPC lipid vesicle attachment, indicating high surface coverage and antifouling properties (final Δf and ΔD shifts around ∼ 0 Hz and ∼ 0 × 10^{-6}, respectively) whereas

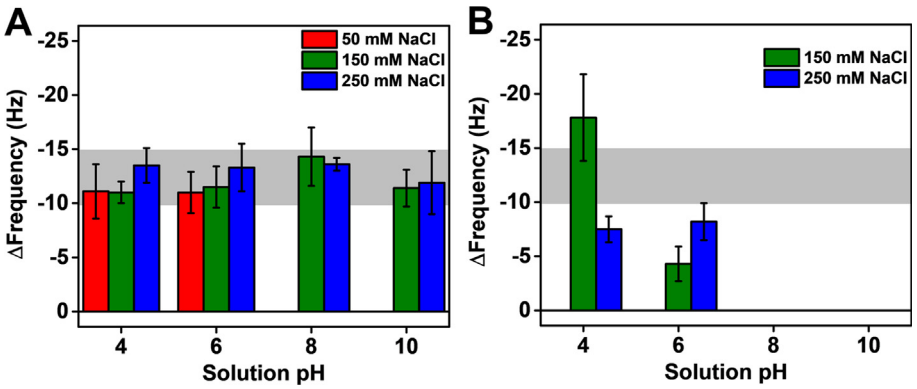

Fig. 6. QCM-D measurement responses for adsorbed DOCP lipid layers after ethanol washing. The frequency, Δf, shifts are reported after adsorbed DOCP lipid layers on **(A)** titania and **(B)** silica were washed with ethanol and then washed again with equivalent buffer solution. The reported Δf shifts are relative to baseline measurements in the appropriate buffer solution before vesicles were added, and correspond to remaining bound lipid. The shaded region of frequency shifts corresponds to the typical range that is expected for a lipid monolayer. The mean and standard deviation are reported from at least three independent experiments.

prodigious adsorption and fusion was observed on the bare surfaces. These findings support that covalently attached DOCP SLBs on titania and noncovalently attached DOCP SLBs on silica both confer antifouling properties while the relative stability of covalent *versus* noncovalent attachment chemistries could be particularly advantageous depending on the application need.

Discussion

From these experimental observations, some insights into the mechanism of DOCP lipid binding to titania and silica surfaces are proposed. Schematic illustrations of possible covalent and noncovalent binding modes are shown in Fig. 7. First, the experimental evidence supports that DOCP lipids strongly attach to the titania surface across all tested pH conditions, as indicated by the general observation that a DOCP lipid monolayer remained attached after ethanol washing. This finding points to covalent attachment ("chemisorption") of DOCP lipids on the titania surface. The only cases where there was negligible DOCP lipid attachment occurred when the ionic strength was low, and therefore repulsive electrostatic interactions between the negatively charged DOCP lipid vesicles and titania surface precluded vesicle adsorption. At pH 6 and below, the phosphate group on the DOCP lipid is singly deprotonated and reacts with the titania surface to likely form a bidentate attachment consisting of two P-O-Ti bonds [61]. Other monodentate and tridentate attachment schemes are possible but the popular consensus of experimental [61,62] and computational [63] studies is that bidentate attachment is energetically preferable in terms of stability and sterics. The bidentate attachment mode is

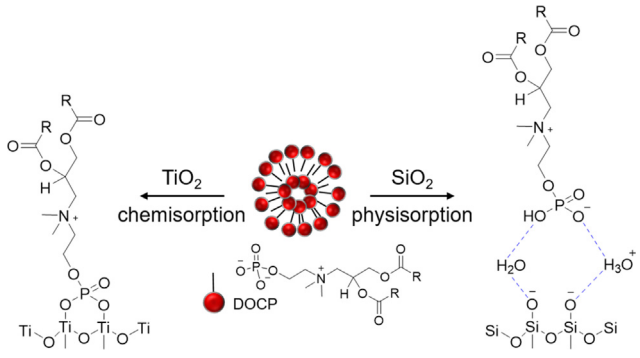

Fig. 7. Covalent and noncovalent binding modes of DOCP lipid to titania and silica surfaces. R denotes generic alkyl chains, in this case $CH_3(CH_2)_7CHCH(CH_2)_6$.

further supported by X-ray photoelectron spectroscopy (XPS) experiments that showed similar phosphate-functionalized amphiphiles also bind to titania-coated QCM-D sensor chips with a bidentate arrangement *via* formation of two P-O-Ti bonds [64]. In this acidic pH regime, the reaction occurs more quickly because the DOCP lipid vesicles and titania surface have relatively low negative zeta potentials [65] and hence there is less electrostatic repulsion and more favorable vesicle adsorption. At higher pH values, the covalent reaction still proceeds but it likely occurs more slowly because there is greater electrostatic repulsion hindering initial adsorption; the phosphate group on the DOCP lipid is doubly deprotonated and both the vesicles and titania surface have larger negative zeta potential values. Indeed, Holt *et al.* reported that alkylphosphate attachment on titania surfaces is slower at pH 7 than pH 4.5 but the resulting film stability is greater at pH 7 (Ref. [65]).

Hence, DOCP lipid binding to titania depends on both noncovalent and covalent forces, demonstrating the importance of taking into account both the vesicle adsorption step and subsequent chemical reaction step. The final chemistry of DOCP lipid attachment to the titania surface is thus mediated by covalent bond formation and hence the lower leaflet of the DOCP SLB is immobile [34]. Indeed, it is remarkable that covalent DOCP lipid attachment can occur even in basic conditions as it has been reported that the contact angle on titania-coated QCM-D sensor chips decreases from > 30° in the pH 4–6 range to < 5° in the pH 8–10 range [66], which is consistent with an enhanced repulsive steric-hydration force in basic conditions to partially counteract the strong van der Waals force [15]. Consequently, in basic conditions, no adsorption occurs at low ionic strength and intact vesicle adsorption or slow SLB formation occurs at high ionic strength.

As such, DOCP SLBs on titania surfaces are well-suited to antifouling applications (as illustrated above) where lateral lipid mobility is not a prerequisite and also have the advantage of supporting hybrid lipid bilayer formation whereby the upper leaflet can be exchanged to modify the lipid composition (*e.g.*, in order to incorporate a ligand-modified lipid headgroup in the upper leaflet for binding detection applications [33]). One particular industrial application where DOCP lipid coatings might be useful would be as corrosion inhibitors for titanium-based medical implant surfaces (see, *e.g.*, other examples of covalently attached molecular layers acting as corrosion inhibitors [67]), in which case the lipid coating would also enhance biomimetic character and potentially biocompatibility of the material interface.

The experimental results obtained on silica are quite distinct from the titania case, and indicate that vesicle adsorption strongly

depends on the solution pH. The low amount of bound DOCP lipid after ethanol washing further supports that the interactions are noncovalent and driven by "physisorption". Interestingly, DOCP lipid attachment only occurred under acidic conditions where both the vesicles and silica surface have smaller negative zeta potentials, and hence there is less electrostatic repulsion. It is also possible that hydronium ions are coordinated at the silica surface and play a role in the binding process, either through ionic or hydrogen bonding interactions. On the other hand, vesicle adsorption is negligible at pH 8 and above due to the increasingly negative zeta potential of the silica surface as well as the electric field of the deprotonated surface hydroxyl groups, which is sufficient to align interfacial water molecules and form an "ice-like" hydration layer [68–70]. It has also been previously reported that the contact angle on silica-coated QCM-D sensor chips decreases from ~10° in the pH 4–6 range to ~6° or lower in the pH 8–10 range [66], which is consistent with enhanced steric hydration repulsion in basic conditions. As such, DOCP lipid binding to silica surfaces is driven by noncovalent forces and occurs preferably at high ionic strength conditions where charge-repulsion is minimized, agreeing well with literature findings that charge is more important than chemical coordination on silica [71]. The ability to functionalize silica surfaces with noncovalently attached DOCP SLBs suggests that they could be useful as antifouling coatings, especially in combination with orthogonal biomodification strategies and perhaps exhibit other biomimetic properties as well.

To contextualize these findings, we also wish to draw comparison between the pH-dependent adsorption behavior of DOCP lipid vesicles *versus* traditionally studied phosphatidylcholine (PC) lipid vesicles on silica and titania surfaces. On silica surfaces, zwitterionic PC lipid vesicles of comparable size readily form noncovalently attached SLBs at pH 4, 6, and 8 but only adsorb without rupture to form an intact vesicle layer at pH 10 (refs. [12,21]). In marked contrast, DOCP lipid vesicles form noncovalently attached SLBs on silica surfaces in sufficiently high ionic strength conditions at pH 4 and 6 but otherwise exhibit negligible adsorption in lower ionic strength conditions at those pH values as well as negligible adsorption in all tested ionic strength conditions at pH 8 and 10.

On titania surfaces, zwitterionic PC lipid vesicles adsorb without rupture to form intact vesicle layers at pH 6, 8, and 10, and exhibit incomplete vesicle rupture at pH 4 due to stronger vesicle-surface interactions (and completely rupture to form an SLB at pH 2.5) [21]. On the other hand, DOCP lipid vesicles can readily form covalently attached SLBs on titania surfaces at pH 4 and 6 and in sufficiently high ionic strength conditions at pH 8 (provided vesicle-surface interactions are not too repulsive to prevent initial vesicle contact). This comparative perspective highlights the unique adsorption behavior of DOCP lipid vesicles on silica and titania surfaces, not only in terms of pH dependency but also due to the effects of ionic strength and it is the interplay of solution pH and ionic strength that influences the self-assembly fabrication outcome.

In the latter scope, it is important to note how these findings advance molecular-level understanding of DOCP lipid vesicle interactions with silica and titania surfaces and lead to new fabrication possibilities. In addition to modulating DOCP lipid vesicle adsorption behavior on titania surfaces, a key novelty of the present work lies in the demonstrated ability to fabricate DOCP SLB coatings on silica surfaces for the first time. Before the present study, the most relevant results reported in the literature discussed how DOCP lipid vesicles do not form SLBs on silica nanoparticle surfaces in 100 mM NaCl at pH 3, 7 or 10 [71]. Indeed, the prevailing notion based on the accumulated experimental evidence to date was that DOCP lipid vesicles do not form SLBs on silica surfaces [30,32,71] while our findings in this study demonstrate that careful tuning of the solution pH and ionic strength in tandem can enable noncovalently attached SLB fabrication on silica surfaces as well.

Conclusion

Our results demonstrate that solution pH and ionic strength play important roles in driving DOCP lipid vesicle adsorption behavior on two widely studied oxide surfaces and that modulating these factors can promote SLB formation when desired. On titania, it was observed that DOCP lipid vesicles can adsorb with or without subsequent rupture, or there was minimal adsorption depending on the specific environmental conditions. Under acidic pH conditions, SLB formation on titania was favorable, while higher ionic strengths were required to promote vesicle adsorption and/or SLB formation under basic pH conditions. In all observed cases, DOCP lipid attachment to titania was driven by covalent bonding events, as indicated by the presence of an apparent lipid monolayer after ethanol washing. On the other hand, a more select set of environmental conditions was identified in which DOCP lipid vesicles can adsorb and spontaneously rupture to form an SLB on silica. In general, higher ionic strength conditions promoted greater lipid attachment due to charge-shielding. This study demonstrates a viable method to fabricate DOCP SLBs on silica while it was also observed that DOCP lipid attachment to silica is weaker and modulated by noncovalent forces. Taken together, our findings highlight the vast surface functionalization possibilities for coating oxide surfaces with phosphonic acid-functionalized lipid monolayers and bilayers, and emphasize the importance of considering both covalent and noncovalent forces when designing DOCP lipid platforms.

Declaration of Competing Interest

The authors declare that they have no known competing financial interests or personal relationships that could have appeared to influence the work reported in this paper.

Acknowledgements

This work was supported by the National Research Foundation of Singapore through a Proof-of-Concept grant (NRF2015NRF-POC0001-19), by the Ministry of Education (MOE) in Singapore under grants RG111/20 and RG34/22, and by the National Research Foundation of Korea (NRF) grants funded by the Korean government (MSIT) (Nos. 2020R1C1C1004385, 2021R1A4A1032782, and 2022K1A3A1A39085112). In addition, this work was supported under the framework of international cooperation program managed by the National Research Foundation of Korea (2022K2A9A2A12000287, FY2022) and by the Basic Science Research Program through the National Research Foundation of Korea (NRF) funded by the Ministry of Education (No.RS-2023-00246169). This work was also partially supported by the SKKU Global Research Platform Research Fund, Sungkyunkwan University, 2023.

Appendix A. Supplementary material

Supplementary data 1. Supplementary data to this article can be found online at https://doi.org/10.1016/j.jiec.2023.07.053.

References

[1] E.T. Castellana, P.S. Cremer, Surf. Sci. Rep. 61 (2006) 429–444.
[2] J. van Weerd, M. Karperien, P. Jonkheijm, Adv. Healthc. Mater. 4 (2015) 2743–2779.

[3] F. Mazur, M. Bally, B. Städler, R. Chandrawati, Adv. Colloid Interface Sci. 249 (2017) 88–99.
[4] T.N. Sut, B.K. Yoon, W.-Y. Jeon, J.A. Jackman, N.-J. Cho, Appl. Mater. Today 25 (2021) 101183.
[5] K. Glasmästar, C. Larsson, F. Höök, B. Kasemo, J. Colloid Interface Sci. 246 (2002) 40–47.
[6] C.-J. Huang, N.-J. Cho, C.-J. Hsu, P.-Y. Tseng, C.W. Frank, Y.-C. Chang, Biomacromolecules 11 (2010) 1231–1240.
[7] C.A. Keller, B. Kasemo, Biophys. J. 75 (3) (1998) 1397–1402.
[8] R.P. Richter, A.R. Brisson, Biophys. J. 88 (2005) 3422–3433.
[9] J.A. Jackman, N.-J. Cho, Langmuir 36 (2020) 1387–1400.
[10] K. Dimitrievski, B. Kasemo, Langmuir 25 (16) (2009) 8865–8869.
[11] K. Dimitrievski, Langmuir 26 (5) (2010) 3008–3011.
[12] K.H. Biswas, J.A. Jackman, J.H. Park, J.T. Groves, N.-J. Cho, Langmuir 34 (2018) 1775–1782.
[13] E. Reimhult, F. Höök, B. Kasemo, Langmuir 19 (2003) 1681–1691.
[14] J.A. Jackman, B. Špačková, E. Linardy, M.C. Kim, B.K. Yoon, J. Homola, N.-J. Cho, Chem. Commun. 52 (2016) 76–79.
[15] J.A. Jackman, G.H. Zan, Z. Zhao, N.-J. Cho, Langmuir 30 (2014) 5368–5372.
[16] A.R. Ferhan, J.A. Jackman, N.-J. Cho, Phys. Chem. Chem. Phys. 19 (2017) 2131–2139.
[17] J.A. Jackman, V.P. Zhdanov, N.-J. Cho, Langmuir 30 (2014) 9494–9503.
[18] T. Rajh, N.M. Dimitrijevic, M. Bissonnette, T. Koritarov, V. Konda, Chem. Rev. 114 (2014) 10177–10216.
[19] N.-J. Cho, S.-J. Cho, K.H. Cheong, J.S. Glenn, C.W. Frank, J. Am. Chem. Soc. 129 (2007) 10050–10051.
[20] M.D. Mager, B. Almquist, N.A. Melosh, Langmuir 24 (2008) 12734–12737.
[21] N.-J. Cho, J.A. Jackman, M. Liu, C.W. Frank, Langmuir 27 (2011) 3739–3748.
[22] L. Zhu, D. Gregurec, I. Reviakine, Langmuir 29 (2013) 15283–15292.
[23] F.F. Rossetti, M. Bally, R. Michel, M. Textor, I. Reviakine, Langmuir 21 (2005) 6443–6450.
[24] F.F. Rossetti, M. Textor, I. Reviakine, Langmuir 22 (2006) 3467–3473.
[25] A. Kunze, P. Sjövall, B. Kasemo, S. Svedhem, J. Am. Chem. Soc. 131 (2009) 2450–2451.
[26] Y. Liu, F. Wang, J. Liu, Langmuir 34 (2018) 9337–9348.
[27] E.K. Perttu, A.G. Kohli, F.C. Szoka Jr, J. Am. Chem. Soc. 134 (2012) 4485–4488.
[28] F. Wang, J. Liu, Small 10 (19) (2014) 3927–3931.
[29] J. Liu, Langmuir 32 (18) (2016) 4393–4404.
[30] F. Wang, J. Liu, J. Am. Chem. Soc. 137 (36) (2015) 11736–11742.
[31] F. Wang, X. Zhang, Y. Liu, Z.Y. Lin, B. Liu, J. Liu, Angew. Chem. Int. Ed. 55 (2016) 12063–12067.
[32] T.N. Sut, A.R. Ferhan, S. Park, D.J. Koo, B.K. Yoon, J.A. Jackman, N.-J. Cho, Appl. Mater. Today 29 (2022) 101618.
[33] T.N. Sut, S.W. Tan, W.-Y. Jeon, B.K. Yoon, N.-J. Cho, J.A. Jackman, Nanomaterials 12 (2022) 1153.
[34] S. Meker, O. Halevi, H. Chin, T.N. Sut, J.A. Jackman, E.-L. Tan, M.G. Potroz, N.-J. Cho, Membranes 12 (2022) 361.
[35] S. Li, F. Wang, X. Li, J. Chen, X. Zhang, Y. Wang, J. Liu, ACS Appl. Mater. Interfaces 9 (2017) 17736–17744.
[36] S. Jiang, W. Wang, L. Dong, X. Yan, S. Li, W. Mei, X. Xie, Y. Zhang, S. Liu, X. Yu, Chem.–A Eur. J. 27 (2021) 12589–12598.
[37] S. Li, W. Mei, X. Wang, S. Jiang, X. Yan, S. Liu, X. Yu, Chem. Commun. 57 (2021) 1372–1375.
[38] S. Li, X. Xie, W. Wang, S. Jiang, W. Mei, Y. Zhang, S. Liu, X. Yu, Nanoscale 14 (2022) 2277–2286.
[39] W. Wang, S. Jiang, S. Li, X. Yan, S. Liu, X. Mao, X. Yu, Chem. Mater. 33 (2021) 774–781.
[40] H. Geng, W. Lin, J. Liu, Q. Pei, Z. Xie, J. Mater. Chem. B 11 (24) (2023) 5586–5593.
[41] R.C. MacDonald, R.I. MacDonald, B.P.M. Menco, K. Takeshita, N.K. Subbarao, L.-R. Hu, Biochimica et Biophysica Acta (BBA)-Biomembranes 1061 (2) (1991) 297–303.
[42] B.J. Berne, R. Pecora, Dynamic Light Scattering: With Applications to Chemistry Biology, and Physics, Courier Corporation, 2000.
[43] M. Pegueroles, C. Tonda-Turo, J.A. Planell, F.-J. Gil, C. Aparicio, Biointerphases (2012) 7.
[44] J.-H. Choi, S.-O. Kim, E. Linardy, E.C. Dreaden, V.P. Zhdanov, P.T. Hammond, N.-J. Cho, J. Phys. Chem. B 119 (2015) 10554–10565.
[45] A. Liu, X. Qi, Computational Mol. Biosci. 02 (03) (2012) 78–82.
[46] C. Keller, K. Glasmästar, V. Zhdanov, B. Kasemo, Phys. Rev. Lett. 84 (2000) 5443.
[47] J.A. Jackman, A.R. Ferhan, N.-J. Cho, Chem. Soc. Rev. 46 (2017) 3615–3660.
[48] R. Richter, A. Mukhopadhyay, A. Brisson, Biophys. J. 85 (2003) 3035–3047.
[49] J.A. Jackman, N.J. Cho, M. Nishikawa, G. Yoshikawa, T. Mori, L.K. Shrestha, K. Ariga, Chem.–An Asian J. 13 (2018) 3366–3377.
[50] N.-J. Cho, C.W. Frank, B. Kasemo, F. Höök, Nat. Protoc. 5 (2010) 1096–1106.
[51] I. Reviakine, F.F. Rossetti, A.N. Morozov, M. Textor, J. Chem. Phys. (2005) 122.
[52] M. Kosmulski, J. Colloid Interface Sci. 337 (2) (2009) 439–448.
[53] K. Suttiponparnit, J. Jiang, M. Sahu, S. Suvachittanont, T. Charinpanitkul, P. Biswas, Nanoscale Res. Lett. 6 (2010) 27.
[54] E. Deplazes, D. Poger, B. Cornell, C.G. Cranfield, Phys. Chem. Chem. Phys. 20 (2018) 357–366.
[55] R. Vácha, S.W. Siu, M. Petrov, R.A. Böckmann, J. Barucha-Kraszewska, P. Jurkiewicz, M. Hof, M.L. Berkowitz, P. Jungwirth, J. Phys. Chem. A 113 (2009) 7235–7243.
[56] G.V. Franks, J. Colloid Interface Sci. 249 (1) (2002) 44–51.
[57] J.A. Jackman, Z. Zhao, V.P. Zhdanov, C.W. Frank, N.-J. Cho, Langmuir 30 (2014) 2152–2160.
[58] E.L. Hinrichsen, J. Feder, T. Jøssang, J. Stat. Phys. 44 (1986) 793–827.
[59] J.A. Jackman, J.-H. Choi, V.P. Zhdanov, N.-J. Cho, Langmuir 29 (2013) 11375–11384.
[60] J.A. Jackman, S.R. Tabaei, Z. Zhao, S. Yorulmaz, N.-J. Cho, ACS Appl. Mater. Interfaces 7 (2015) 959–968.
[61] P. Connor, A.J. McQuillan, Langmuir 15 (1999) 2916–2921.
[62] M.I. Tejedor-Tejedor, M.A. Anderson, Langmuir 6 (1990) 602–611.
[63] R. Luschtinetz, J. Frenzel, T. Milek, G. Seifert, J. Phys. Chem. B 113 (2009) 5730–5740.
[64] S.W. Tan, T.N. Sut, W.-Y. Jeon, B.K. Yoon, J.A. Jackman, Appl. Mater. Today 27 (2022) 101444.
[65] S.A. Holt, A.P. Le Brun, A.R. Nelson, J.H. Lakey, RSC Adv. 3 (2013) 2581–2589.
[66] M.F. Cuddy, A.R. Poda, L.N. Brantley, ACS Appl. Mater. Interfaces 5 (2013) 3514–3518.
[67] S. Neupane, P. Losada-Pérez, U. Tiringer, P. Taheri, D. Desta, C. Xie, D. Crespo, A. Mol, I. Milošev, A. Kokalj, F.U. Renner, J. Electrochem. Soc. 168 (5) (2021) 051504.
[68] Q. Du, E. Freysz, Y.R. Shen, Phys. Rev. Lett. 72 (2) (1994) 238–241.
[69] P.S. Cremer, S.G. Boxer, J. Phys. Chem. B 103 (1999) 2554–2559.
[70] J. Kim, G. Kim, P.S. Cremer, Langmuir 17 (2001) 7255–7260.
[71] X. Wang, X. Li, H. Wang, X. Zhang, L. Zhang, F. Wang, J. Liu, Langmuir 35 (2018) 1672–1681.